Source Process of Deep and Intermediate Earthquakes as Inferred from Long-Period P and S Waveforms 2. Deep-focus and Intermediate-depth Earthquakes around Japan

By

Takeshi MIKUMO

Disaster Prevention Research Institute, Kyoto University

Abstract

The dynamical processes at the source of eleven deep-focus and intermediate-depth earthquakes that occurred around Japan have been investigated from the analysis of long-period *P* and *S* waveforms.

The recorded *P* waveforms have been equalized at some distance around the focal region to get the source function, eliminating the combined effects of wave propagation in the earth and of the seismograph characteristics. It is found that the source process times derived from the source function, as well as from the recorded first half-periods, indicate some azimuthal dependence with respect to the orientation of one nodal plane and of the null vector, in most of the earthquakes. This dependence is interpreted as a result of shear faulting over a finite fault area, and used to determine the slip plane, slip direction, fault length and width. The seismic moment and the average dislocation over the plane are evaluated from *P* wave amplitudes together with the estimated fault dimension.

A close agreement in general features between the recorded and synthesized waveforms including the absolute amplitudes of both *P* and *S* waves supports the above shear dislocation model. The overall distribution of the orientations of the slip planes and slip vectors of these earthquakes does not seem to be definitely related to the local dip or strike of seismic zones in this region.

The calculated stress drops during these earthquakes, together with some available data, appear to show a gradual increase with focal depths down to 400 km. A tentative interpretation of this increase is that the stress drop might be related, at least qualitatively, to partial loss of the intrinsic (cohesive) shear strength of the material under increasing hydrostatic pressures, if these earthquakes are caused by brittle fractures in the lithosphere.

§ 1. Introduction

The focal mechanism of a number of deep-focus and intermediate-depth earthquakes around Japan has been extensively investigated (BALAKINA, 1962; ICHIKAWA, 1961, 1966; RITSEMA, 1965; HONDA *et al.*, 1967; KATSUMATA and SYKES, 1969; ISACKS and MOLNAR, 1971), since the pioneering work of HONDA and his colleagues (HONDA *et al.*, 1952, 1956), and their results from the first motion studies made great contributions to clarify the distribution of the earthquake-generating stresses in relation to the tectonic features of deep seismic zones in this region.

Recent seismological approaches, on the other hand, using the spectrum or waveform of body and surface waves with the introduction of shear dislocation models have proved effective to estimate not only the geometrical orientation of a possible fault plane but also more physical source parameters including the source dimension, the amount and direction of slip displacement, its time function, the fracture velocity and the stress-strain drop during deep earthquakes (BERCKHEMER and JACOB, 1968; MIKUMO, 1969, 1971; FUKAO, 1970, 1971; ABE, 1971; WYSS, 1971).

It is the purpose of this paper to elucidate such dynamical processes at the source of deep and intermediate earthquakes around

Japan, and their tectonic implications particularly to deep seismic zones or descending plates of lithosphere around this region. The present approach is to estimate the various source parameters from the recorded P waveforms, and to synthesize three-component seismograms of direct P and S waves on the basis of the inferred source process, taking into account the effects of wave propagation and recording instruments, to compare with the observed records.

§ 2. Data

Analyzed in this study are eleven deep-focus and intermediate-depth earthquakes that occurred around Japan in recent four years from 1967 to 1970 with magnitudes greater than 5.8. The information pertinent to these earthquakes, mainly based on the determinations of the United States National Oceanic and Atmospheric Administration, is tabulated in Table 1. The locations of these earthquakes are shown in Fig. 1, which cover a part of the Kurile-Kamchatka arc, the northeastern Hokkaido, the Sea of Japan, the Izu-Bonin arc and of the Ryukyu arc, and the focal depths range from 140 to 510 km. Light dotted lines indicate approximate depths of the seismic zones taken from ISACKS and MOLNAR (1971). Data mainly used here are the long-period vertical and horizontal component seismograms recorded at the World-wide Standardized Network (WWSSN) stations, and other available information from stations of the Japan Meteorological Agency, high-sensitive university stations inside Japan, and also from seismological bulletins including the Earthquake Data Report, are incorporated to determine the focal mechanism.

§ 3. Focal Mechanism

Figs. 2 (a) and (b) show the radiation pattern of P wave first motions for the eleven earthquakes, each of which includes more than 100 P and PKP data projected onto the lower hemisphere of the Wulff net. Circles are for stations on the lower hemisphere, and triangles correspond to near-by stations on the upper hemisphere projected through the center onto the lower hemisphere. Open symbols (circles and triangles) indicate compressional first motions and solid ones are dilatations. P and T denote the positions of the maximum pressure and tension axes respectively. It may be inferred from the patterns that the focal mechanism of these earthquakes is of the double-couple source or of equivalent shear faulting. It is to be noted that earthquake No. 5, which should be regarded as a multiple shock, includes data for the first small shock mainly from Japanese stations and data for the second large shock mainly from the WWSSN stations. Since the radiation pattern does not

Table 1. Information of the earthquakes analyzed.

Shock No.	Date	Origin time h	m	s	Location φ(N)	λ(E)	Depth km	M	Plane 1 d	dd	Plane 2 d	dd
1	1967 Dec. 1	13	57	02.4	49.5°	154.4°	136	5.9	86°	137°	20°	237°
2	1968 May 14	14	05	06.0	29.9	129.4	168	5.9	76	105	22	23
3	1968 Oct. 7	19	20	20.4	26.3	140.6	516	6.1	50	94	62	210
4	1969 Jan. 19	07	02	04.4	45.0	143.2	204	6.4	54	143	84	240
5	1969 Mar. 31	19	25	27.2	38.3	134.6	417	5.9	80	130	68	35
6	1969 Dec. 18	13	32	46.0	46.3	142.5	344	5.9	68	249	68	151
7	1970 Mar. 23	00	20	54.7	40.1	140.2	146	5.8	21	60	74	280
8	1970 Mar. 23	12	14	53.5	29.8	129.3	148	5.8	58	75	60	183
9	1970 May 27	12	05	06.0	27.2	140.1	382	6.2	28	55	66	200
10	1967 Aug. 13	20	06	50.6	35.3	135.3	357	6.0	75	323	28	202
11	1968 Feb. 28	12	08	01.5	32.9	137.7	349	5.8	86	270	8	35

Remarks: d; dip, dd; dip direction

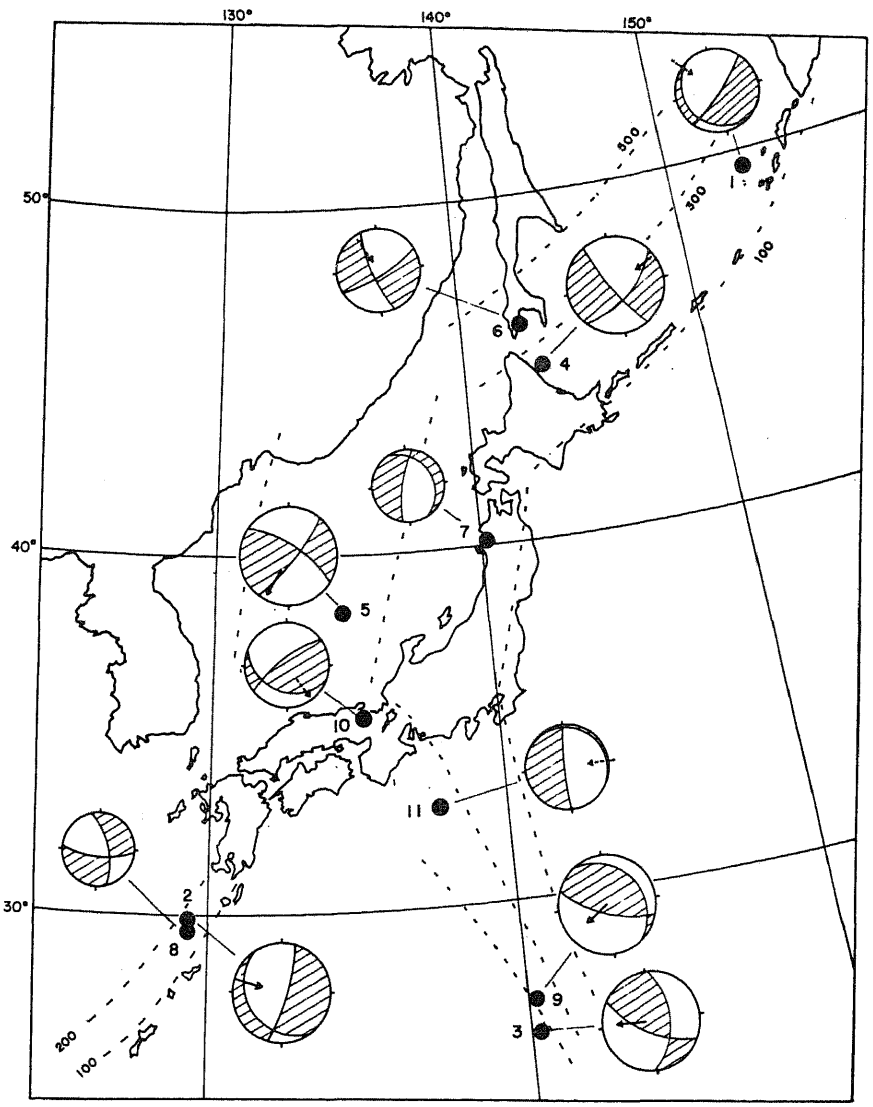

Fig. 1. Locations and the fault-plane solutions of intermediate and deep-focus earthquakes around Japan.

make much difference for these two shocks (OIKE, 1971), the two kinds of data have been superposed here, leaving some inconsistencies. The focal mechanism solutions for the eleven earthquakes are also schematically shown in Fig. 1, in which shaded parts indicate dilatational area. The dip and dip directions of two nodal planes are given in Table 1. The tectonic implications of the mechanism, together with distributions of the inferred slip planes and slip directions will be discussed in a later section.

§ 4. Source Functions, Source Process Times, and Inferences of Source Parameters

In this section, we shall make an attempt to obtain the source functions and to evaluate the apparent time duration of energy release at the source, from the recorded P waveforms. Solid curves on the left-side for each station in Figs. 3 (a) and (b) indicate some examples of the vertical component records of P waves

from earthquakes No. 3 and No. 5, and those in Figs. 6 (a) and (b) show the seismograms for earthquakes No. 2 and No. 9. The recorded waveforms include the effects of the source finiteness $S(\omega)$ and the source time function $\dot{U}(\omega)$, the effects of wave propagation in the mantle $P(\omega)$, and of the crust-mantle structure around the source region $C_M(\omega)$ and around a recording station $C(\omega)$, and the seismograph characteristics $I(\omega)$ (TENG and BEN-MENAHEM, 1965; MIKUMO, 1969).

The seismogram $f(t)$ recorded at the station may therefore be written (MIKUMO, 1969),

$$f(t)=\frac{1}{2\pi}\int_{-\infty}^{\infty}\dot{U}(\omega)\cdot S(\omega)\cdot H(\omega)\,e^{i\omega t}\,d\omega$$
$$=\int_{0}^{\infty}u_0(t')\cdot h((t-t')dt' \qquad (1)$$

where $H(\omega)$ is the overall system tranfer function as defined by $H(\omega)=C_M(\omega)\cdot C(\omega)\cdot P(\omega)\cdot I(\omega)$, and $h(t)$ is the impulse response of the system. If we eliminate, through deconvolution, the entire effects of wave distortion $H(\omega)$ in the linear transmitting system assumed here, the waveforms can be equalized back to some distance near the source region in the following way,

$$u_0(t)=\frac{1}{2\pi}\int_{-\infty}^{\infty}F(\omega)H^{-1}(\omega)e^{i\omega t}\,d\omega$$
$$=\frac{1}{2\pi}\int_{-\infty}^{\infty}\dot{U}(\omega)S(\omega)e^{i\omega t}\,d\omega \qquad (2)$$

and hence this may be understood as the source function.

$F(\omega)$ can be obtained from the Fourier transform of the seismogram $f(t)$. $C_M(\omega)$,

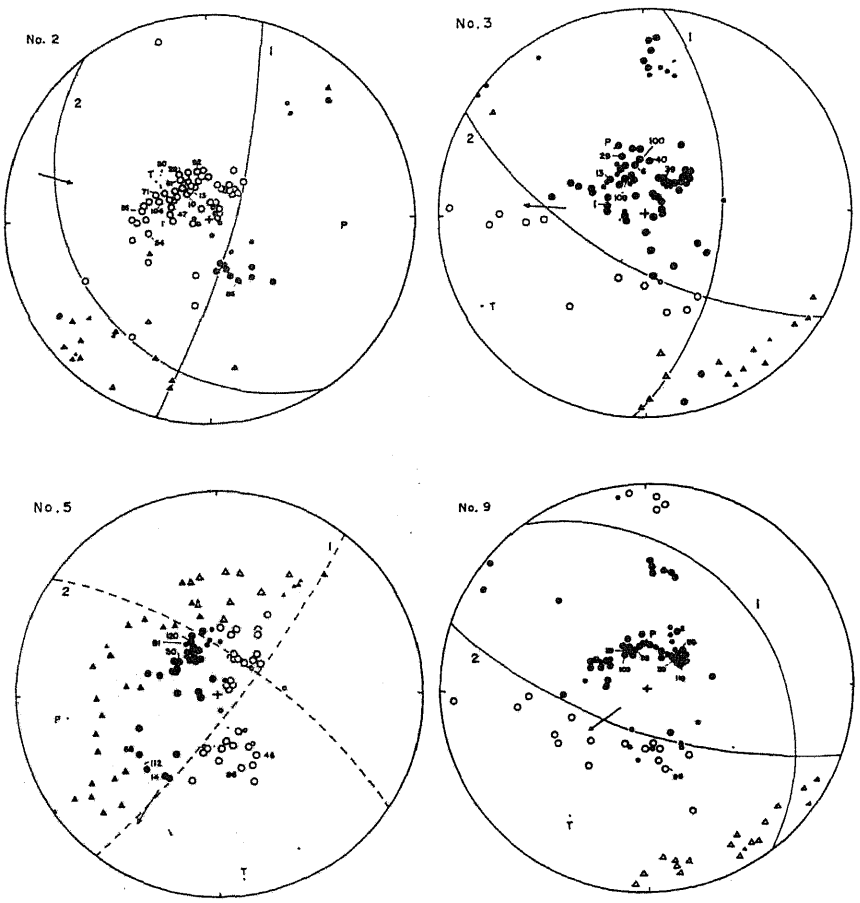

2 (a)

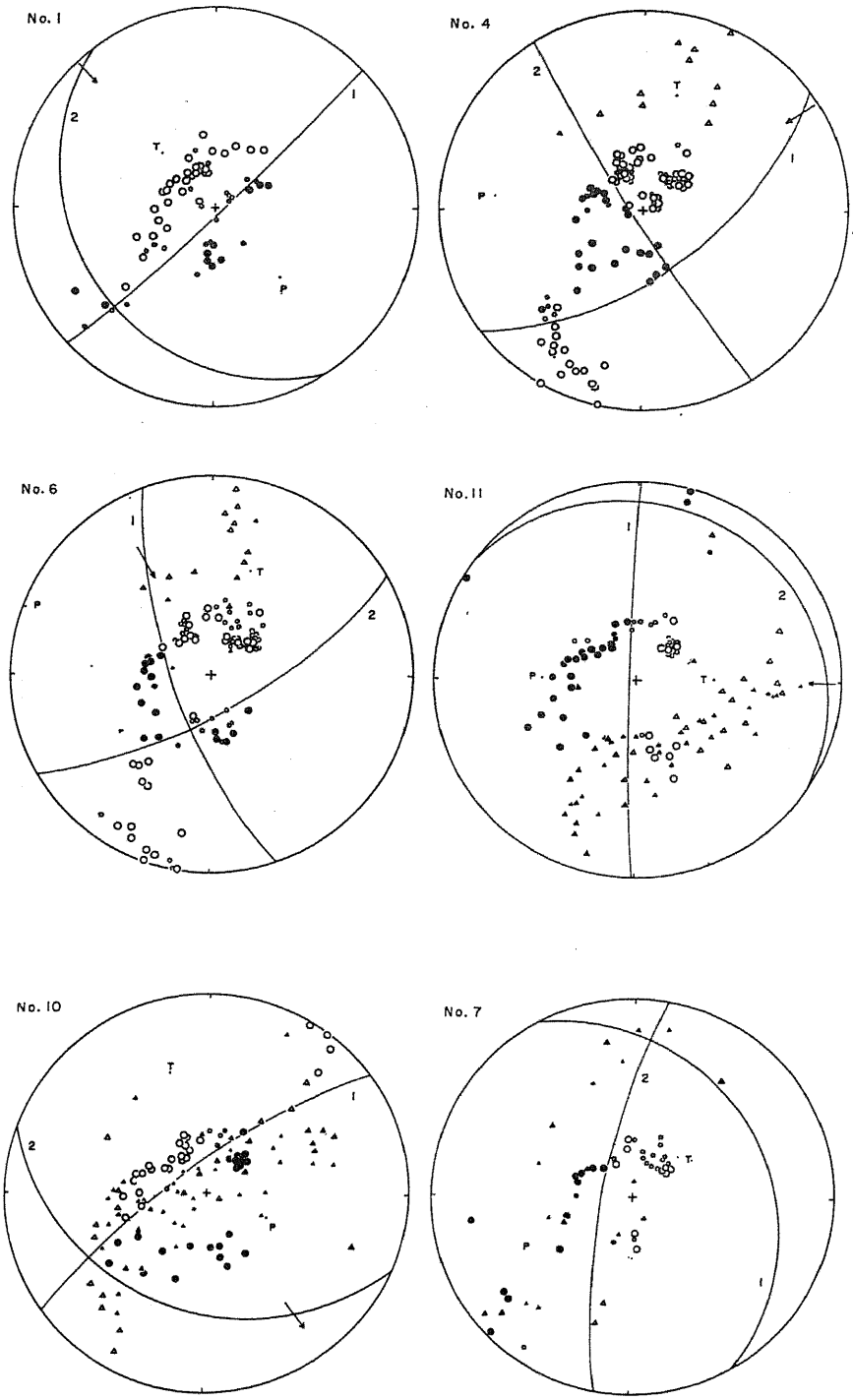

2 (b)

Fig. 2. Fault-plane solutions. open symbols: compression, solid symbols: dilatation, circles: stations on the lower hemisphere, triangles: stations on the upper hemisphere.

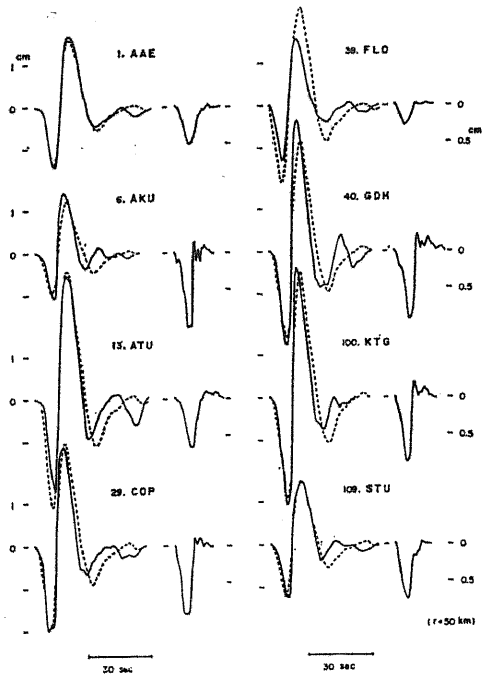

3 (a)

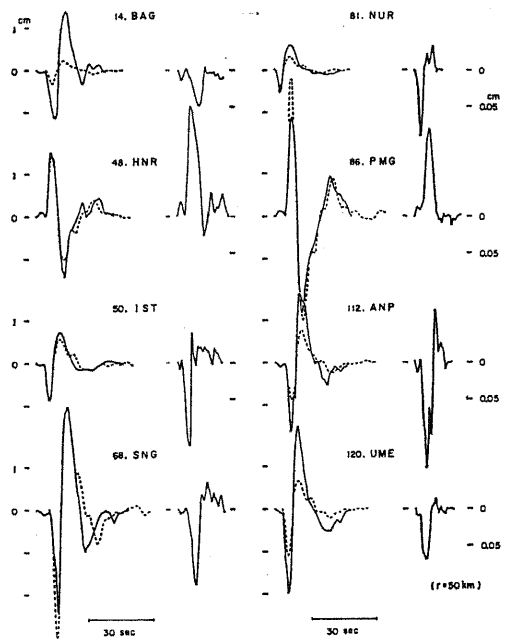

3 (b)

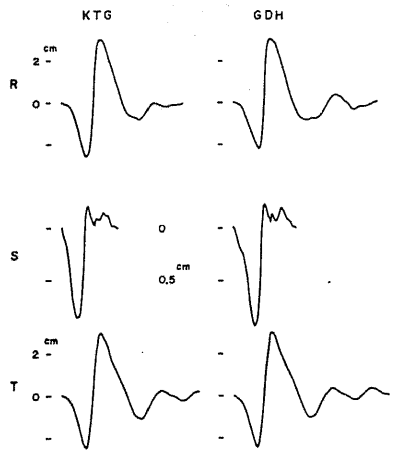

3 (c)

Fig. 3. Recorded (full line) and synthesized (broken line) P waveforms and their equalized source functions. (a) No. 3 (b) No. 5. (c) R: record, S: source function, T: recovered seismogram.

which does not provide important effects for deep earthquakes, has been omitted here. Computations of $P(\omega)$ for the effects of geometrical spreading and attenuations were based on the Jeffreys-Bullen velocity profile and a mantle Q model (Model 11) of MIKUMO and KURITA (1968) including the dispersive effects (FUTTERMAN, 1962). $C(\omega)$ has been computed for the layered structure appropriate to each recording site, but for unilayered model of Haskell when the structure is not well known. $I(\omega)$ was taken from the conventional long-period seismograph system used at the WWSSN. All computations of the transfer functions and Fourier synthesis were made at an interval of 0.005 c/s in the frequency range between 0.005 and 0.1 c/s, and with a logarithmic increment of 1.10 between 0.1 and 1.0 c/s. For the latter frequency range, a high-cut filter with linearly decreasing amplification has been applied to $F(\omega)H^{-1}(\omega)$. To check the reliability of the computed source functions, attempts have been made to recover $f(t)$ from $u_0(t)$ by a convolution technique. It is seen in Fig. 3(c) that the agreement between the original and recovered waveforms appears satisfactory.

The traces in the right-side in Figs. 3 (a) and (b) are the source functions equalized at a distance of 50 km, all of which have a

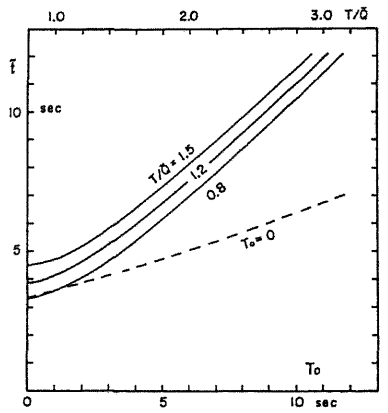

Fig. 4. Relation between the assumed source process times and the times of the first half-cycle of P waves on the synthesized seismograms.

wedge-like form similar to those obtained by BERCKHEMER and JACOB (1968) for the ground motion. As can be seen in Fig. 3 (b), the source functions for earthquake No. 5 are preceded by a small shock. It will now be directly noticed that the breadth of the base of these functions, which are termed hereafter the source process time T_0, bears some differences depending on the location of the stations.

The source process times may also be estimated from the time of the first half-cycle of the recorded P waves, using the following empirical relations (BOLLINGER, 1968; MIKUMO, 1971). Fig. 4 shows the relations between T_0 and $\tilde{t}$ established on a number of hypothetical, synthetic seismograms, which have been constructed by the convolution of $u_0(t)$ for variously assumed values of T_0 with the impulse response $h(t)$ for a variety of attenuation effects. A number of trial calculations show that allowance for the instrumental constants, T_s=13—17 sec, T_g=90—100 sec, h_s =0.8—1.5, h_g=0.8—1.5 and σ^2=0.0—0.1, yield differences in $\tilde{t}$ less than 0.4 sec. It has also been confirmed that the source process times thus estimated from the recorded first half-periods agree, to a satisfactory accuracy, with those on the calculated source functions.

In order to examine a possible azimuthal dependence of the source process times estimated for eight earthquakes, T_0 and $\tilde{t}$ are plotted in Figs. 5 (a) and (b) against three directions $\alpha_{1,2,3}$; the direction cosines of a seismic ray with respect to the normal to two nodal planes and to the null vector, respectively. It can be seen that there are some dependence, but with rather large scatter, between T_0 and α_1 and also between T_0 and α_3 for shocks Nos. 2, 3 and 9, and also dependence between T_0 and α_2 and between T_0 and α_3 for shock No. 5. For the other four shocks, Nos. 1, 4, 6 and 11, similar but weaker dependence may be recognized, but it was no longer possible to find this dependence for earthquakes with smaller magnitudes.

The azimuthal dependence of the source process times may be interpreted by a shear dislocation model with finite dimension. In this model, the source function can be written (MIKUMO, 1971),

$$\left.\begin{aligned} u_0(t) &= \int_0^\infty \Delta\dot{u}(t')\cdot s(t-t')\mathrm{d}t' \\ \text{where} \\ \Delta\dot{u}(t) &= D[H(t)-H(t-\tau)]/\tau \\ s(t) &= S_0\int_0^\infty s_L(t')\cdot s_W(t-t')\mathrm{d}t' \\ s_{L,W}(t) &= [H(t)-H(t-2T_{L,W})]/2T_{L,W} \end{aligned}\right\} \quad (3)$$

and hence the source process time or the breadth of the base of the function is,

$$\begin{aligned} T_0 &= \tau+2(T_L+T_W) \\ &= \tau + L\left|\frac{1}{v_L}-\frac{\alpha_j}{v_p}\right| + W\left|\frac{1}{v_W}-\frac{\alpha_k}{v_p}\right| \end{aligned} \quad (4)$$

where $S_0=(LW/2\pi v_p)(v_s/v_p)^2\alpha_1\alpha_2$, L and W are the length and width of the slip plane, D is the average dislocation on the fault surface, τ is the rise time of dislocation, v_L and v_W are the apparent fracture velocities along the directions of L and W, and v_p and v_s are the compressional and shear velocities around the source region. Applying the above relation to our observations in Fig. 5, we can conclude that the nodal plane including the null vector and the normal relevant to the dependence corresponds to the slip plane. The direction of slip motion is oriented parallel to the normal passing through the pole of the other nodal plane, and its sense can be determined from the compression and dilatation pattern of P wave first motions. The slip vector

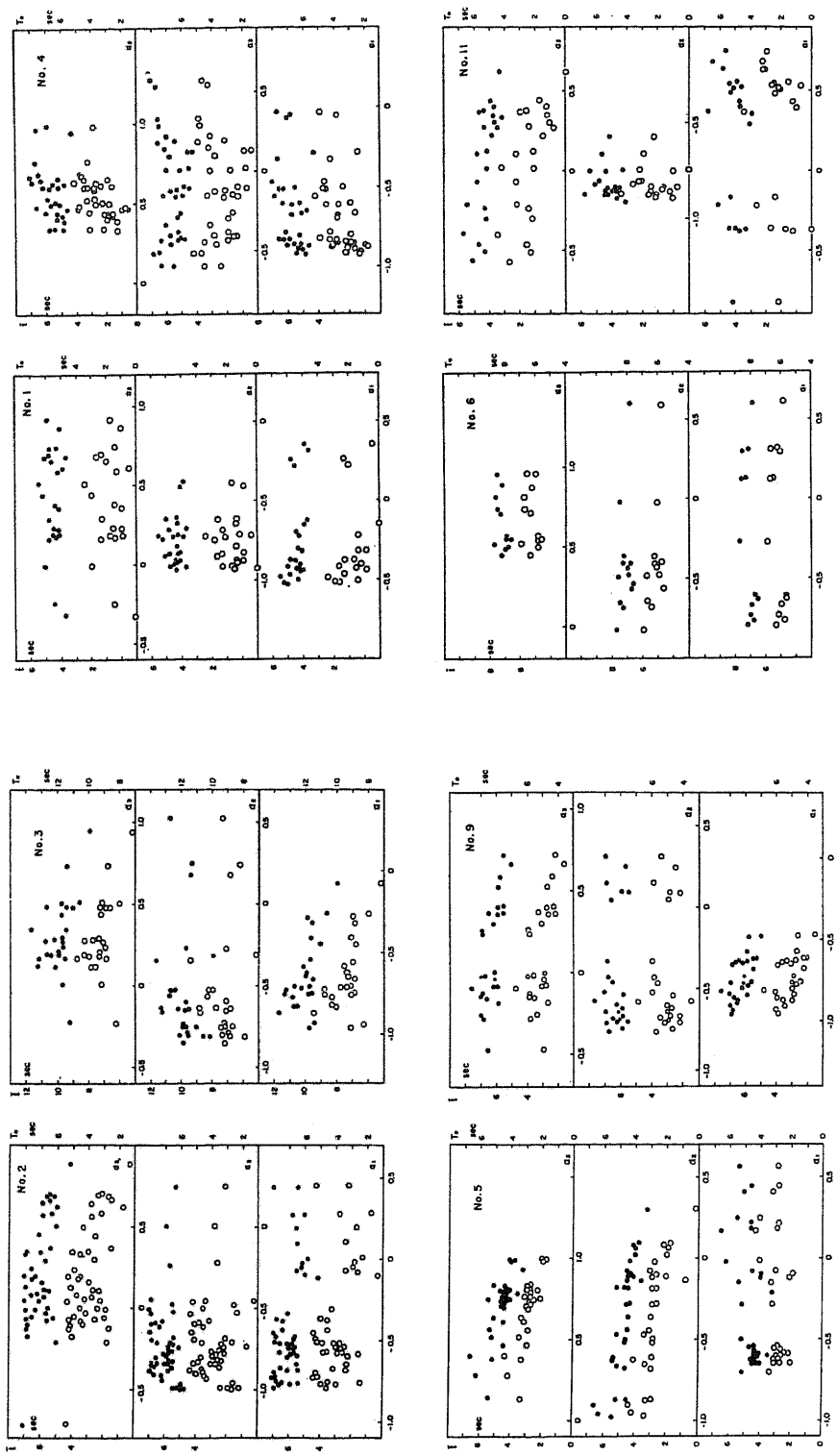

5 (a) 5 (b)

Fig. 5. Azimuthal dependence of the source process times (open circles) and the first half-periods (solid circles). (a) Nos. 2, 3, 5, and 9 (b) Nos. 1, 4, 6, and 11.

thus determined is indicated by arrows in Figs. 1 and 2. The source dimensions L and W have been evaluated by least squares from eq. (4), rearranging the signs of $\alpha_{j,k}$ and assigning an appropriate value to v_p. The estimated values with uncertainty for eight earthquakes are summarized in Table 2. The time constant of dislocation and the direction and velocity of fracture propagation along the slip plane cannot be uniquely determined without further assumptions, since the least squares yield only the intercept time $t_s=\tau\pm L/v_L\pm W/v_W$. Assumptions of $v_L=v_W=v$ and $\tau=0$ (step-function type) do not lead to reasonable values of the fracture velocity for most of the earthquakes. If we assume here bidirectional faulting (MIKUMO, 1971) travelling in a direction of 45° ($v_L=v_W=v/0.7$) and $v\cong 0.9\,v_s$ (4.9—4.8 km/sec), τ would take values between 0.1—0.5 sec for five earthquakes, and 1.9, 3.6 and 5.8 sec for earthquake Nos. 4, 3 and 6 respectively. The large τ values for the last three shocks might also be understood from a blunt onset of P waveforms.

§ 5. Observed and Synthesized Seismograms

We shall next calculate synthesized seismograms of both P and S waves and compare them with the corresponding records, to test the validity of the shear dislocation models assumed here. Theoretical seismograms of P waves have been synthesized in such a way as expressed in eq. (1), with the estimated source dimensions and assumed time constant and fracture velocities. Figs. 6(a) and (b) show examples of the observed and synthesized seismograms of the vertical component of P waves for earthquakes No. 2 and No. 9. In Figs. 3(a) and (b) are also displayed the two kinds of seismograms for earthquakes No. 3 and No. 5 respectively. Comparison of the P wave amplitudes in the time domain between the two kinds of seismograms provides the seismic moment M_0 and hence the dislocation D. This assigns the absolute values to the theoretical amplitudes. Figs. 7(a) and (b) show the relationship between the theoretical and observed double amplitudes for the eight earthquakes. Most of the plotted points

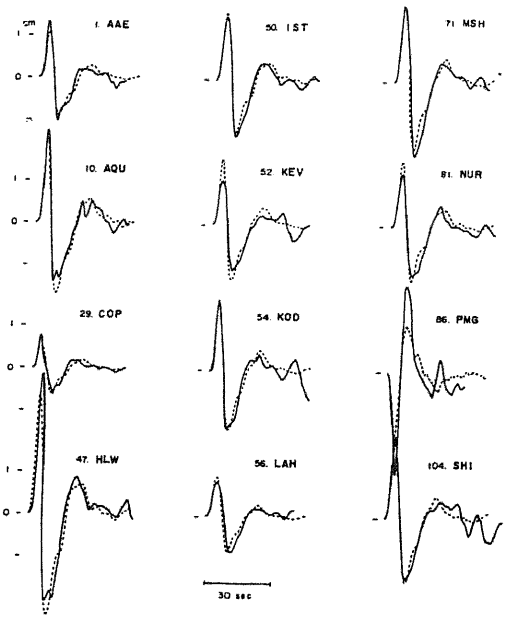

6 (a)

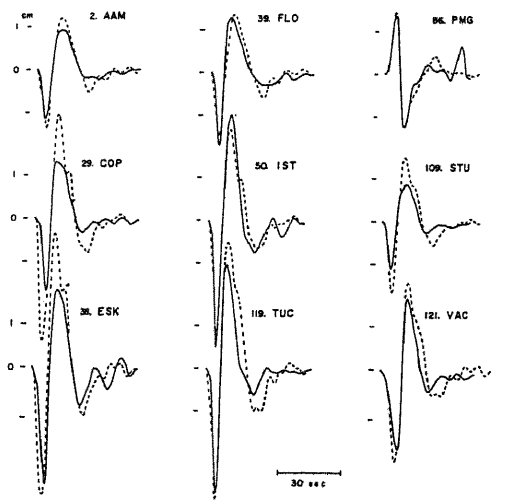

6 (b)

Fig. 6. Examples of the recorded (full line) and synthesized (broken line) vertical component seismograms of P waves. (a) No. 2 (b) No. 9.

fall along a straight line, indicating that the P wave amplitudes as well as their waveforms may be well explained by the inferred model.

Theoretical seismograms of SV and SH waves can be synthesized in a similar way, with the parameters estimated from P waves

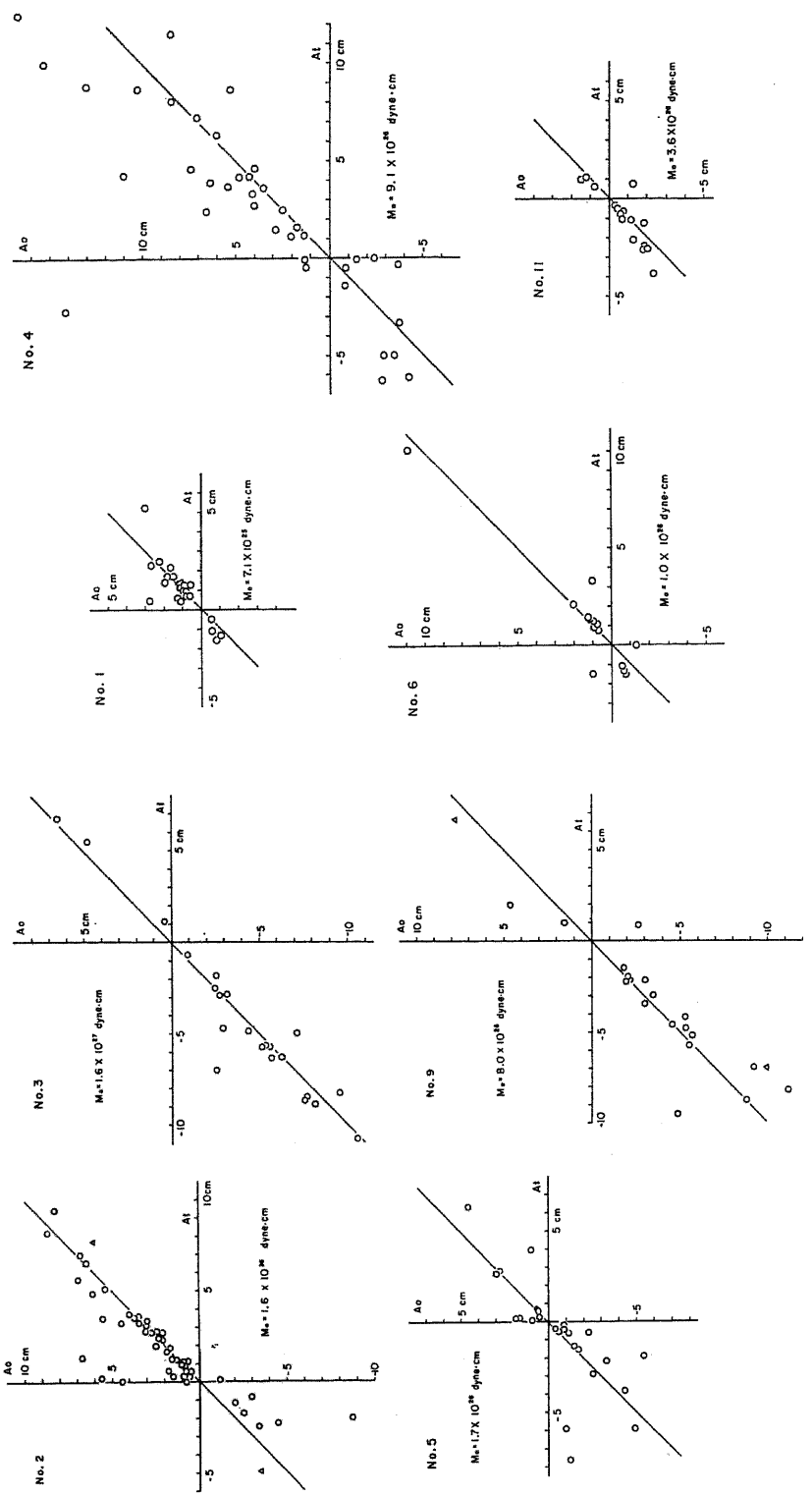

7 (a) 7 (b)

Fig. 7. Relation between the double amplitudes of P waves on the recorded and synthesized seismograms. (a) Nos. 2, 3, 5, and 9 (b) Nos. 1, 4, 6, and 11.

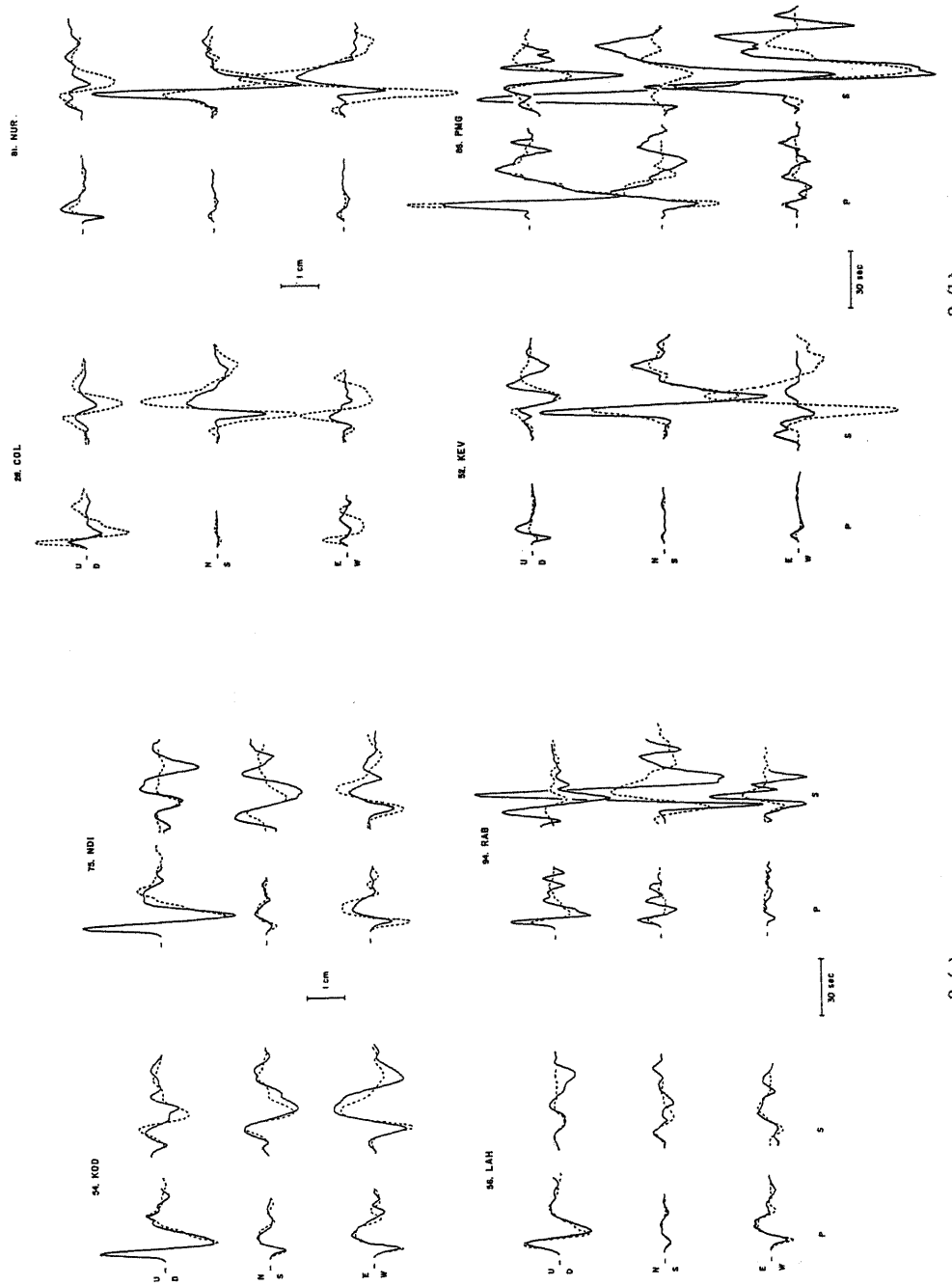

8 (a) 8 (b)

Fig. 8. Examples of the recorded (full line) and synthesized (broken line) three-component seismograms of P and S waves. (a) No. 2 (b) No. 5.

and the S wave amplification factors due to the focal mechanism, taking into account the mantle transfer function (divergence and attenuation with $Q_\beta=4/9\,Q_\alpha$) and the crustal response appropriate to S waves (MIKUMO, 1971). The SV and SH waves are resolved into the NS and EW components to compare directly with the corresponding records, although this comparison can be made only for a limited number of stations due to difficulty of selecting well-isolated direct S waves. Figs. 8 (a) and (b) depict the observed and synthesized three-component seismograms of P and S waves. It appears that general features of the three components show satisfactory agreement in the case of earthquake No. 2, except for one component at a station. For earthquake No. 5, however, there are appreciable differences between the computed and observed amplitudes. This may be due partly to uncertainty in the focal mechanism solution and partly to contamination from later phases, and lateral variations of attenuations.

§ 6. Discussion

It may be concluded from the foregoing results that the radiation pattern of P wave first motions, azimuthal dependence of the source process times, and satisfactory agreement in the waveforms including the absolute amplitudes between the observed and synthesized seismograms of P and some of S waves, all favor, at least to a first approximation, the shear dislocation models for these deep earthquakes around Japan. It is to be noted, however, that a volumetric source subjected to sudden change in shear modulus due to phase transitions could also generate wave radiations equivalent to the double-couple type (KNOPOFF and RANDALL, 1970), and there could be small fraction of addi tional component to the double-couple force (RANDALL and KNOPOFF, 1970).

Orientation of Stresses and Slip Planes

The focal mechanism solutions in Fig. 1 obtained for earthquakes No. 1, Nos. 7 and 5, Nos. 10 and 11, and Nos. 9 and 3 appears consistent with the general pattern described by ISACKS and MOLNAR (1971) in regions of the Kamchatka-Kurile arc, North Honshu, the junction between the Izu-Boinin arc and North Honshu, and of the Izu-Bonin arc, respectively. The mechanism for earthquake No. 1 and No. 10 has also been reported independently by them, indicating a good agreement with our solutions, although ours include much more data from near stations. The above solutions suggest that the pressure axis (down-dip compression) tends to be parallel to the dip of seismic zones or descending lithosphere plate in the last three regions, as has been pointed out by ICHIKAWA (1961, 1966) and ISACKS and MOLNAR (1971), and that the parallelism holds for the tension axis (down-dip extension) in the first region. Solutions for Nos. 4 and 6 in the Hokkaido corner and for No. 2 in the Ryukyu arc show, however, somewhat different patterns from ISACKS and MOLNAR (1971), and consistent rather with the solutions by HONDA *et al.* (1956) and ICHIKAWA (1966), and by KATSUMATA and SYKES (1969), respectively. These exceptions might be associated with complicated tectonic structures such as oblique-angled junctions, contortions of the lithosphere and so on (ISACKS and MOLNAR, 1971).

In Fig. 1 are indicated by arrows the possible slip planes and the slip directions of the upper block relative to the lower one, which have been inferred from the present analysis. Broken arrows means somewhat questionable choice of the fault plane because of weak azimuthal variations of the source process times, and there could be another choice in these cases. It is to be noted that the slip plane of earthquake No. 5 agrees with that determined by OIKE (1971) from the travel time differences of first P waves from the double shocks of this earthquake. It appears that there is no systematic trend in the overall distribution of the inferred slip planes and slip directions related to tectonic structures such as local dip or strike of seismic zones around this region.

Close examinations of the five reliable solutions show, however, that the slip planes or slip directions of earthquakes No. 4 and No. 5 in the northern Honshu, with a predominant

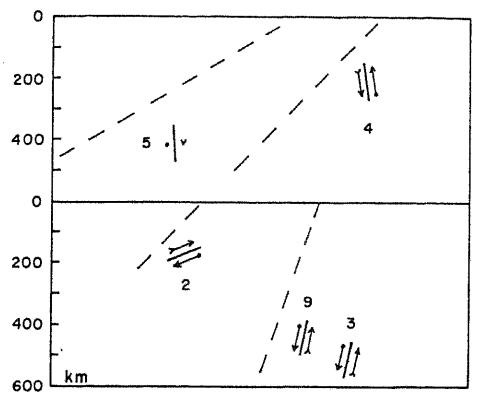

Fig. 9. Schematic representation of the orientation of slip planes and the local dip of seismic zones.

strike-slip component, are oriented almost parallel to the strike of the seismic zones, but that earthquake No. 9, 3 and 2 in the south of Honshu, which are characterized by predominant dip-slip component, have a slip direction nearly normal to the strike of the seismic zones. In order to examine possible relations between the orientation of the slip plane or the slip direction and the local dip of the presumed lithospher plate, the five fault-plane solutions are schematically shown in Fig. 9, on the cross section of the seismic zones. Small solid circles and wings on the rear end of arrows indicate strike-slip motion towards up and away down seen from this paper sheet respectively. This may also be understood from Fig. 1. Broken oblique lines at the left side of each shock show the local dip of seismic zone in the respective regions (ISACKS and MOLNAR, 1971), but do not indicate the periphery of the zone. This figure suggests that the orientation of the slip plane and slip directions relative to the seismic zone appreciably differ for these earthquakes, indicating almost pure strike-slip (No. 5), reverse faulting (No. 4), underthrusting (No. 2) and normal faulting (Nos. 3 and 9), respectively.

This variety of slip motions would be explained neither by the hypothesis of SUGIMURA and UYEDA (1967), who associate the formation of a fault plane with a preferred orien-

Table 2. Estimated source parameters.

Source parameters	No. 1	No. 2	No. 3	No. 4	No. 5	No. 6	No. 9	No. 11
Focal depth h (km)	136	168	516	204	417	344	382	349
Seismic Moment M_0 (10^{26} dyne·cm)	0.71	1.56	15.6	9.05	1.68	1.03	8.00	0.36
Fault length L (km)	9-12	12-14	24-30	17-22	10-14	8-12	24-30	14-17
Fault width W (km)	5- 8	10-13	8-14	18-24	5-10	<7	6-8	<4
Dislocation D (cm)	1.0-2.3	1.2-1.8	3.3-7.5	2.3-3.8	1.5-3.9	1.6-3.1	4.0-6.7	>1.6
Stress drop $\Delta\sigma$ (bars) 1)	175-302	160-283	440-620	174-381	300-441	378-661	550-758	171-300
2)	81-124	69-126	202-286	81-147	106-152	156-270	297-334	118-144

Stress drop 1) calculated from ESHELBY (1957) and KEYLIS-BOROK (1959)
2) calculated from CHINNERY (1969)

tation of olivine crystals in the upper mantle, nor by generation of a nearly horizontal fault plane parallel to pre-existing weakness (SAVAGE, 1969).

Source Parameters

Table 2 summarizes the estimated source parameters for the eight larger earthquakes analyzed here. The seismic moment differ appreciably for these earthquakes with magnitudes between 5.8 and 6.4. The fault length ranges from 10 to 30 km, somewhat smaller than that for intermediate-depth earthquakes with comparable moments in the southwest Pacific region (MIKUMO, 1971). The average fault width is about 8–10 km, but it reaches a comparable order with the fault length for three intermediate earthquakes, Nos. 1, 2 and 4. This suggests a possibility that faulting for these earthquakes could be bilateral or circular rather than pure unilateral. It would also be possible to interpret the $T_0 \sim \alpha_1$ plot for the first two earthquakes and $T_0 \sim \alpha_2$ plot for earthquake No. 4 as having azimuthal variations symmetric to $\alpha_j = 0$, which are expected for bilateral faulting. The amount of dislocation is found to be 1–7 m, which appears considerably larger than that for shallow earthquakes with comparable moments. (MOLNAR and WYSS, 1972).

The stress drop has been calculated by $\Delta\sigma = (7/16)M_0/r^3$ for dislocations with a circular crack (ESHELBY, 1957; KEYLIS-BOROK), which is assumed to be able to apply to these earthquakes with an equivalent radius r, and also for dislocations with a rectangular fault plane ($L \times W$) (CHINNERY, 1969) from $\Delta\sigma = (2M_0/3\pi)(4/L^2 + 3/W^2)/(L^2 + W^2)^{1/2}$. It is most appropriate to refer to the latter in the present case, but the former has been used for the sake of comparison with available data. Although the estimated values have rather large uncertainty according to precision of the fault area, the lower bounds corresponding to the possible largest fault dimensions may be accepted as most reliable ones. Since the smaller fault width evaluated by least squares are less reliable except for earthquakes No. 2 and No. 4, we tentatively take here the larger fault width multiplied by the smaller fault length as the lower bounds of the fault area. The calculated stress drops under the two assumptions are given in Table 2, where we see that a circular fault assumption yields almost twice the values from a rectangular fault. In Fig. 10 the center values with their probable ranges of the stress drop from the first assumption are plotted against focal depths, together with those obtained by

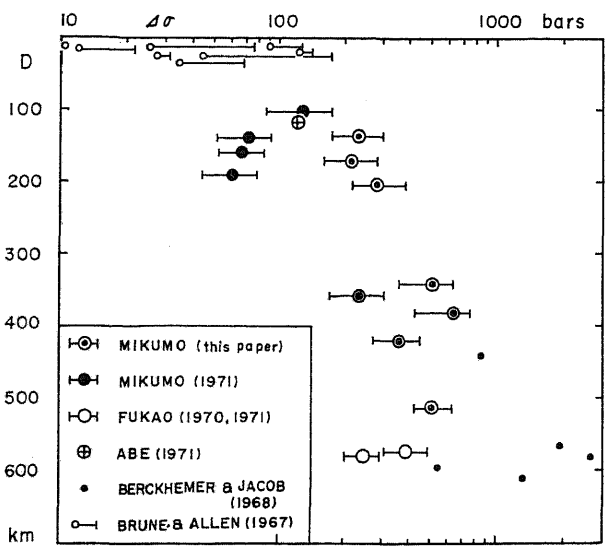

Fig. 10. Estimated stress drops against focal depths.

BERCKHEMER and JACOB (1968) and FUKAO (1970, 1971) for deep-focus earthquakes, by MIKUMO (1971) and ABE (1971) for intermediate-depth earthquakes, and those compiled by BRUNE and ALLEN (1967) for shallow earthquakes. The values by the first authors, which are unfortunately based on an erroneously replaced divergence factor, have been corrected here, and we take the values only for five shocks with more than seven data. Tabulated values by the last authors (marked by small open circles) which are from an indefinitely long vertical or horizontal fault, have also been corrected (the right end of lines) for circular cracks to compare with the other observations. Although the stress drop might be a function of seismic moment and could be subjected to regional differences as suggested by MOLNAR and WYSS (1972) for shallow earthquakes, we notice here that the estimated values for deep earthquakes are several times larger than those for shallow earthquakes, and that they tend to increase with depth down to about 400 km. If they are plotted against hydrostatic pressures at appropriate depths, a linear relation with rather large scatter apply. This is the case even if we refer to CHINNERY (1969) for stress drop calculation for all the earthquakes. WYSS (1971) recently calculated the source parameters of deep earthquakes in the Tonga arc from the corner frequency of body wave spectra using BRUNE's theory (1970), and also found larger stress drop at intermediate depths than at shallow crust.

A Consideration on the apparent increase in stress drop with depth

Larger stress drops for deep earthquakes result apparently from smaller fault dimension and/or larger displacements on the slip plane, but there might be more substantial significance. A tentative interpretation is described here.

One would expect that the stress drop during seismic faulting may be directly associated with the average shear strength of rock material in the earth's crust and mantle (e.g. CHINNERY, 1964). Laboratory experiments (e.g. GRIGGS and HANDIN, 1960; MOGI, 1966) show, however, that the shear strength of rocks under high confining pressures corresponding to hydrostatic pressures in the lower crust reaches several kilobars, two orders of magnitudes larger than the estimated stress drops. This evidence suggests that the stress released during earthquakes is only a small fraction of the total stress supported by the rock around faults (PRESS and BRACE, 1966). This would be the case for intermediate and deep-focus earthquakes, but it has been pointed out that increased hydrostatic pressures and elevated temperatures in the upper mantle do not allow dry frictional sliding (OROWAN, 1960), and would not yield ordinary Coulomb-type brittle fracture as in shallow earthquakes (GRIGGS and HANDIN, 1960) but rather an increase of ductility or uniform flow (GRIGGS *et al.*, 1960; HEARD, 1960). On the other hand, however, the experiments of RALEIGH and PATTERSON (1965) suggest the possibility that brittle fractures could occur even under such environments due to dehydration of hydrous minerals. This phenomenon has been explained by weakening of the shear strength or decrease of the principal shear stress required to cause failure due to the role of interstitial fluid pressures, as expressed in a modified form of the Coulomb-Mohr failure condition, $\tau=\tau_0+\mu(\sigma-p)$ (HUBBERT and RUBEY, 1959), where σ is the normal stress or confining pressure across the fracture plane, p the pore pressure with $p=\lambda\sigma$ $(0<\lambda<1)$, τ_0 the shear strength of the material in case of zero normal stress, and μ is the coefficient of internal friction. ISACKS *et al.* (1968), MCKENZIE (1969), and ISACKS and MOLNAR (1969, 1971) have suggested that intermediate and deep-focus earthquakes are caused by brittle fractures within descending cold slabs of the lithosphere when compressional or extensional stress resulted from gravitational force acting on the slab exceeds the strength of the material.

We tentatively assume here that the shear stress to produce faulting in the lithosphere may be approximately specified by the modified failure condition, since there is a possibility that released water from hydrous

minerals, partially molten magma, or some vapour from them exist even in the lower portion of the lithosphere, under a possible temperature distribution lower by about 500°C than that in the surrounding mantle (e.g. HASEBE, 1970), although there are arguments against this interpretation (e.g. GRIGGS and BAKER, 1969). Faulting process will initiate at a point where the shear stress first overcome the local shear strength of the lithosphere. Once fracture has started at some point, complete or partial loss of the intrinsic cohesive strength τ_0 will follow (HUBBERT and RUBEY, 1959; GRIGGS and HANDIN, 1960; BERG, 1968), and hence the shear stress required for further faulting will drop as, $\tau_2=(1-\gamma)\tau_0+\mu_2(\sigma-p)$. The stress drop would then be, $\Delta\tau=\tau_1-\tau_2=\gamma\tau_0+(\mu_1-\mu_2)(1-\lambda)\sigma$, where γ $(0<\gamma<1)$ is the fraction of the loss, μ_1 and μ_2 may be regarded as the static and kinetic coefficients of internal friction.

τ_0 estimated for various rocks from laboratory experiments at room temperatures ranges from a few hundreds bars to about a few kilobars (e.g. HANDIN and HAGER, 1957; JAEGER, 1959; MOGI, 1966), still one order of magnitude greater than the intercept of our $\Delta\tau$-hydrostatic pressure relation. The discrepancies might be due partly to a decrease of τ_0 with increasing temperatures (MATSUSHIMA, 1961; TOWLE and RIECKER, 1968), partial loss of the cohesive strength (GRIGGS and HANDIN, 1960), and by the size effect of material (e.g. MOGI, 1966b; and references in material mechanics), which would come from the existence of microscopic flaws in rocks in the real earth. The coefficient of internal friction μ_1 in brittle regime depends weakly on confining pressures (MOGI, 1966) and temperatures (TOWLE and RIECKER, 1968), but takes values of the order of 10^{-1} to 10^{0}, so that the difference $\mu_1-\mu_2$ would be one or two orders of magnitude lower than μ_1. Thus, it appears that the apparent increase of the estimated stress drops with hydrostatic pressures and hence with focal depths down to 400 km may be accounted for, at least qualitatively, by the experimental failure condition. This is not inconsistent with some experimental results (e.g. MATSUSHIMA, 1966) that the ratio of stress drop to applied initial stress becomes smaller for stronger medium, since the absolute values of applied stress or hydrostatic pressures in the present case increase with depth.

Alternative hypotheses such as shear melting instability (GRIGGS and HANDIN, 1960; GRIGGS and BAKER, 1969), or lubrication due to partial melting (SAVAGE, 1969), and creep instability (OROWAN, 1960) have been presented to account for the physical properties of deep earthquakes. In those cases, the stress drop would be associated with the cohesive strength of partially molten material between fault faces, as that of soil-like materials in shallow earthquakes (BERG, 1968), or creep strength of material there. Since the order of the strengths seems plausible to compare with seismic stress drops, these possibilities cannot be rule out at this stage.

It should be emphasized that the above interpretations involving many assumptions are only tentative, and it is undoubtedly necessary to analyze much more deep earthquakes, to examine and regional and depth variations of stress drops as well as of slip vectors of fault planes.

Acknowledgments

I wish to thank Dr. Peter Molnar for comments on this study, Drs. Kazuo Oike, Katsuyuki Abe, Michio Otsuka and Shogo Matsushima for discussions on many problems. My thanks are also due Mrs. Ritsuko Koizumi for assistance in the present work. Seismograms were supplied by the United States National Oceanic and Atmospheric Administration, and computations were made on a FACOM 230-60 at the Data Processing Center, Kyoto University.

References

Abe, K., Source studies of intermediate-depth earthquakes based on long-period seismic waves, 1. The South Sandwich Islands earthquake of May 26, 1964, *Phys. Earth and Planet. Intr.*, 1972 (in press).

Balakina, L. M., General regularities in the direction of the main stresses acting in the earhthquake foci of the Pacific seismic belt, Izv. Akad. Nauk.

SSSR. ser. geophys. (Engl. Transl.), 918-926, 1962.
Berckhemer, H. and K.H. Jacob, Investigation of the dynamical process in earthquake foci by analyzing the pulse shape of body waves, Proc. Xth Assembly, ESC, 1968, II, 253-352, 1970.
Bollinger, G.A., Determination of earthquake fault parameters from long-period P waves, *J. Geophys. Res.*, **73**, 785-807, 1968.
Brune, J. and C.R. Allen, A low stress-drop, low magnitude earthquake with surface faulting: The Imperial, California, earthquake of March 4, 1966, Bull. Seism, Soc. Amer., **57**, 501-514, 1967.
Brune, J., Tectonic stress and spectra of seismic shear waves from earthquakes, *J. Geophys. Res.*, **75**, 4997-5009, 1970.
Chinnery, M.A., Theoretical fault models, Publ. Dominion Obs., Ottawa, **37**, 211-223, 1969.
Eshelby, J.D., The determination of the elastic field of an ellipsoidal inclusion and related problems, *Proc. Roy. Soc.*, London, **A241**, 376-396, 1957.
Fukao, Y., Focal process of a deep-focus earthquake as deduced from long-period P and S waves, *Bull, Earthq. Res. Inst.*, **48**, 707-727, 1970.
Fukao, Y., Focal process of a large deep-focus earthquake as inferred from long-period P waves —The western Brazil earthquake of 1963—, Phys. Earth and Planet. Intr., 1972 (in press).
Futterman, W.I., Dispersive body waves, *J. Geophys. Res.*, **67**, 5279-5291, 1962.
Honda, H., and A. Masatsuka., On the mechanism of earthquakes and the stresses producing them in Japan and its vicinity, *Sci. Rep., Tohoku Univ.*, Ser. 5, Geophys., **4**, 42-60, 1952.
Honda, H., A. Masatsuka, and K. Emura, On the mechanism of earthquakes and the stresses producing them in Japan and its vicinity (2nd paper), *Sci. Rep., Tohoku Univ.*, Ser. 5, Geophys., **8**, 186-205, 1956.
Honda, H., A. Masatsuka, and M. Ichikawa, On the mechanism of earthquakes and stresses producing them in Japan and its vicinity (third paper), *Geophys. Mag.*, **33**, 271-279, 1967.
Ichikawa, M., On the mechanism of the earthquake in and near Japan during the period from 1950 to 1957, *Geophys. Mag.*, **30**, 355-403, 1961.
Ichikawa, M., Mechanism of earthquakes in and near Japan, 1950-1962, *Papers in Meteorol. and Geophys.*, **16**, 201-229, 1966.
Isacks, B., J. Oliver, and L.R. Sykes, Seismology and the new global tectonics, *J. Geophys. Res.*, **73**, 5855-5899, 1968.
Isacks, B. and P. Molnar, Mantle earthquake mechanism and the sinking of the lithosphere, *Nature*, **223**, 1121-1124, 1969.
Isacks, B. and P. Molnar, Distribution of stresses in the descending lithosphere from a global survey of focal mechanism solutions of mantle earthquakes, *Rev. Geophys.*, **9**, 103-174, 1971.
Katsumata, M. and L.R. Sykes, Seismicity and tectonics of the western Pacific: Izu-Mariana-Caroline and Ryukyu-Taiwan regions, *J. Geophys. Res.*, **74**, 5923-5960, 1969.
Keylis-Borok, V.I., On estimation of the displacement in an earthquake source and of source dimensions, *Ann. Geofis.*, **12**, 205-214, 1959.
Knopoff, L. and M.J. Randall, The compensated linear-vector dipole: a possible mechanism for deep earthquakes, *J. Geophys. Res.*, **75**, 4957-4963, 1970.
McKenzie, D.P., Speculations on the consequences and causes of plate motions, *Geophys. J.*, **18**, 1-32, 1969.
Mikumo, T. and T. Kurita, Q distribution for long-period P waves in the mantle, *J. Phys. Earth*, **16**, 11-29, 1968.
Mikumo, T., Long-period P waveforms and the source mechanism of intermediate earthquakes, *J. Phys. Earth*, **17**, 169-192, 1969.
Mikumo, T., Source process of deep and intermediate earthquakes as inferred from long-period P and S waveforms, 1. Intermediate-depth earthquakes in the southwest Pacific region, *J. Phys. Earth*, **19**, 1-19, 1971.
Molnar, P. and M. Wyss, Moments, source dimensions and stress drops of shallow-focus earthquakes in the Tonga-Kermadec arc, Phys. Earth and Planet. Intr., 1972 (in press).
Oike, K., On the nature of the occurrence of intermediate and deep earthquakes 3. Focal mechanism of multiplets, Bull. *Disaster Prevention Res. Inst., Kyoto Univ.*, **21**, 153-178, 1971.
Randall, M.J. and L. Knopoff, The mechanism at the focus of deep earthquakes, *J. Geophys. Res.*, **75**, 4965-4976, 1970.
Ritsema, A.R., The mechanism of some deep and intermediate earthquakes in the regions of Japan, *Bull. Earthq. Res. Inst.*, **43**, 39-52, 1965.
Teng, T.L. and A. Ben-Menahem, Mechanism of deep eartdquakes from spectrums of isolated dody wave signals, 1. Banda Sea earthquake of March 21, 1964, *J. Geophys. Res.*, **70**, 5157-5170, 1965.
Wyss, M., Source parameters of intermediate and deep focus earthquakes in the Tonga arc, presented at a symposium of the XV General Assembly of the IUGG, Moscow, 1971.

References added in § 6.

Berg, C.A., Relation between stress drop, fault

friction, and crustal strength in shallow focus strike slip faulting, *J. Geophys. Res.*, **73**, 2217–2223, 1968.

Chinnery, M. A., The strength of the earth's crust under horizontal shear stress, *J. Geophys. Res.*, **69**, 2085–2089, 1964.

Griggs, D. T., F. J. Turner and H. C. Heard, Deformation of rocks at 500 to 800°C, in Rock Deformation, *Geol. Soc. Amer.*, Memoir **79**, 39–104, 1960.

Griggs, D. T. and J. Handin, Observation on fracture and a hypothesis of earthquakes, *ditto*, 347–364, 1960.

Griggs, D. T. and D. W. Baker, The origin of deep-focus earthquakes, in The Properties of Matter, 23–42, *John Wiley and Sons, New York*, 1969.

Handin, J. and R. V. Hager, Experimental deformation of rocks under confining pressure: Tests at room temperature on dry samples, *Amer. Assoc. Petrol. Geol. Bull.*, **41**, 1–50, 1957.

Hasebe, K., N. Fujii and S. Uyeda, Thermal process under island arcs, *Tectonophysics*, **10**, 335–355, 1970.

Heard, H. C., Transition from brittle to ductile flow in Solenhofen limestone as a function of temperature, confining pressure, and interstitial fluid pressure, in Rock Deformation, *Geol. Soc. Amer.*, Memoir **79**, 39–193, 1960.

Hubbert, M. K. and W. W. Rubey, Role of fluid pressure in mechanics of overthrust faulting I., *Bull. Geol. Soc. Amer.*, **70**, 115–166, 1959.

Jaeger, J. C., Elasticity, fracture and flow, with engineering and geological applications, *John Wiley and Sons, New York*, 1964.

Matsushima, S., On the strength distribution of the earth's crust and the upper mantle, and the distribution of the great earthquakes with depth, *Bull. Disaster Prev. Res. Inst., Kyoto Univ.*, **43**, 1–12, 1961.

Matsushima, S., Fracture of rocks in solid medium: A consideration of the occurrence of the earthquake sequences, *Spec. Contr. Geophys. Inst., Kyoto Univ.*, **6**, 289–301, 1966.

Mogi, K., Pressure dependence of rock strength and transition from brittle fracture to ductile flow, *Bull. Earthq. Res. Inst.*, **44**, 216–232, 1966a.

Mogi, K., Some precise measurements of fracture strength of rocks under uniform compressive stress, *Rock Mech. and Eng. Geol.*, **4**, 41–55, 1966b.

Orowan, E., Mechanism of seismic faulting, in Rock Deformation, *Geol. Soc. Amer.*, Memoir **79**, 323–345, 1960.

Press, F. and W. F. Brace, Earthquake prediction, Science, **152**, 1575–1584, 1966.

Raleigh, C. B. and M. S. Patterson, Experimental deformation of serpentinite and its tectonic implications, *J. Geophys. Res.*, **70**, 3965–3985, 1965.

Savage, J. C., The mechanics of deep-focus faulting, *Tectonophysics*, **8**, 115–127, 1969.

Sugimura, A. and S. Uyeda, A possible anisotropy in the upper mantle accounting for deep earthquake faulting, *Tectonophysics*, **5**, 25–33, 1967.

Towle, L. C. and R. E. Riecker, The pressure and temperature dependence of the shear strength of minerals, *J. Appl. Physics*, **39**, 4807–4811, 1968.

(Received Oct. 1, 1971;
revised Dec. 28, 1971)